New model and scheme for compressible fluids of the finite difference lattice Boltzmann method and direct simulations of aerodynamic sound

Tsutahara, Michihisa
Kataoka, Takeshi
Shikata, Kenji
Takada, Naoki

(Citation)
Computers and Fluids,37(1):79-89

(Issue Date)
2008-01

(Resource Type)
journal article

(Version)
Accepted Manuscript

(URL)
https://hdl.handle.net/20.500.14094/90000996

New Model and Scheme for Compressible Fluids of the Finite Difference Lattice Boltzmann Method and Direct Simulations of Aerodynamic Sound

M. Tsutahara [1]*, T. Kataoka[1], K. Shikata[2], N.Takada[3]

[1] Graduate School of Science and Technology, Kobe University, 1-1 Rokkodai-machi, Nada, Kobe, 657-8501, Japan
[2] Graduate School of Science and Technology, Kobe University, 1-1 Rokkodai-machi, Nada, Kobe, 657-8501, Japan
[3] National Institute of Advanced Industrial Science and Technology, 16-1 Onogawa, Tsukuba, 305-8569, Japan
[1*] Tel: +81-78-803-6137, e-mail: tutahara@mech.kobe-u.ac.jp,

Abstract

A new scheme for the finite difference lattice Boltzmann method is proposed, in which negative viscosity term is introduced to reduce the viscosity and the calculation time can be remarkably reduced for high Reynolds number flows. A model with additional internal degree of freedom is also presented for diatomic gases such as air, in which an additional distribution function is introduced. Direct simulations of aero-acoustics by using the proposed model and scheme are presented. Speed of sound is correctly recovered. As typical examples, the Aeolian tone emitted by a circular cylinder is successfully simulated even very low Mach number flow. Full three-dimensional sound emission is also given

Key words: Lattice Boltzmann method, Finite difference method, Direct simulation aero-acoustics, Aeolian tone, Three-dimensional sound emission.

1. Introduction

The lattice Boltzmann method is now a very powerful tool of computational fluid dynamics (CFD). This method is different from ordinary Navier-Stokes equations based CFD methods, and is based on the particle motions [1]-[9]. Historically, this method has been developed from the lattice gas method (LGM) or lattice gas automaton (LGA) [1]-[3], but it is also derived from the Boltzmann equation, which is a basic equation of the molecular gas dynamics, and can be considered a strongly discretized version of the Boltzmann equation [10], [11].

However, mostly successful model so far is for incompressible fluids, and only a few simulations by the models for compressible or thermal-fluid model have been reported. Several models for thermal compressible models have been proposed, for example Alexander et al. [12], Chen et al. [13], and Takada et al. [14]. In lattice Boltzmann method, on the other hand, the mode of energy of the fluid particle is limited to that due to translation. Then the ratio of the specific heats is given by

$$\gamma = \frac{D+2}{D} \tag{1}$$

where D represents the space dimension, and in two-dimensional flows $\gamma = 2$, which is unrealistic and even for three-dimensional flows $\gamma = 5/3$, which will be applicable to monatomic gases only but not to the most important diatomic gas, that is air.

In this paper, two- and three-dimensional models for thermal compressible fluids, including internal degree of freedom and having variable specific heats is introduced based on Takada's model [15], and apply the models to the finite difference lattice Boltzmann method [16]. A new lattice BGK equation, by which the calculation can be performed with larger time increment, is also introduced. Some typical aero-acoustics, Aeolian tone and edge tone, are simulated by this model.

2. Finite difference lattice Boltzmann method

The equation to be solved is the following discretized Bhatnager-Gross-Krook (BGK) equation[14]

$$\frac{\partial f_i(t,\mathbf{r})}{\partial t} + c_{i\alpha}\frac{\partial f_i(t,\mathbf{r})}{\partial r_\alpha} = -\frac{1}{\phi}\left[f_i(t,\mathbf{r}) - f_i^{(0)}(t,\mathbf{r})\right] \tag{2}$$

where f_i is the particle distribution function at time t and position $\mathbf{r}$, subscripts i represents the direction of particle translation and α the Cartesian co-ordinates, $f_i^{(0)}$ on the RHS is the local equilibrium distribution function, $\mathbf{c}_i$ is the particle velocity, and ϕ is called the single relaxation time factor. In this equation, the representative particle velocity c is chosen unity and the representative time increment τ is also chosen unity. In the form of the differential equations, f_i does not represent the state of the lattice site as in the conventional lattice Boltzmann method but the continuous variable in the physical time-space field.

The macroscopic variables for continuous fluids are given from f_i taking the moments of $\mathbf{c}_i$ as:

Density $\rho = \sum_i f_i$ (3)

Momentum $\rho u_\alpha = \sum_i f_i c_{i\alpha}$ (4)

Energy $\frac{1}{2}\rho u^2 + \rho e = \sum_i \frac{1}{2} f_i c_i^2$ (5)

where e is the internal energy per unit mass. The constraints that determine the form of the local equilibrium distribution function are

Density $\rho = \sum_i f_i^{(0)}$ (6)

Momentum $\rho u_\alpha = \sum_i f_i^{(0)} c_{i\alpha}$ (7)

Energy $\frac{1}{2}\rho u^2 + \rho e = \sum_i \frac{1}{2} f_i^{(0)} c_i^2$ (8)

Momentum flux: $p\delta_{\alpha\beta} + \rho u_\alpha u_\beta = \sum_i f_i^{(0)} c_{i\alpha} c_{i\beta}$ (9)

Energy flux: $\left(\frac{1}{2}\rho u^2 + \rho e\right) u_\alpha = \sum_i \frac{1}{2} f_i^{(0)} c_i^2 c_{i\alpha}$ (10)

Definition of the variables in the same forms by particle distribution function in (3) to (5), and its local equilibrium state in (6) to (8) means that to the above variables, mass, momentum and energy of the fluid particle, are conserved in the collision stage.

The local equilibrium distribution function can be defined as

$$f_a^{(0)} = F_a \rho \left[1 - 2B(\mathbf{c}_a \cdot \mathbf{u}) + 2B^2(\mathbf{c}_a \cdot \mathbf{u})^2 + B(\mathbf{u} \cdot \mathbf{u}) - \frac{4}{3} B^3 (\mathbf{c}_a \cdot \mathbf{u})^3 - 2B^2 (\mathbf{c}_a \cdot \mathbf{u})(\mathbf{u} \cdot \mathbf{u}) \right] \tag{11}$$

where subscript a represents the kind of particles and their moving directions, and will be written as $a = p,k,i$, and p and k are given in Tables.1 and 2 for two- and three-dimensional flows, respectively. The constants are determined for two-dimensional flows as follows [14].

$$F_0 = 1 + \frac{5}{4Bc^2}\left(\frac{17}{96B^2c^4} + \frac{35}{48Bc^2} + \frac{49}{45}\right) \tag{12a}$$

$$F_{11} = -\frac{1}{8Bc^2}\left(\frac{13}{16B^2c^4} + \frac{71}{24Bc^2} + 3\right) \tag{12b}$$

$$F_{12} = \frac{1}{16Bc^2}\left(\frac{5}{16B^2c^4} + \frac{25}{24Bc^2} + \frac{3}{5}\right) \tag{12c}$$

$$F_{13} = -\frac{1}{24Bc^2}\left(\frac{1}{16B^2c^4} + \frac{1}{8Bc^2} + \frac{1}{15}\right) \tag{12d}$$

$$F_{21} = \frac{1}{4B^3c^6}\left(\frac{Bc^2}{3} + \frac{1}{8}\right) \tag{12e}$$

$$F_{22} = -\frac{1}{1536B^3c^6}\left(2Bc^2 + 3\right) \tag{12f}$$

$$B = -\frac{1}{2e} \tag{12g}$$

For three-dimensional case, these constants are [14]

$$F_0 = 1 + \frac{1}{8Bc^2}\left(\frac{287}{80B^2c^4} + \frac{1549}{120Bc^2} + \frac{49}{3}\right) \tag{13a}$$

$$F_{11} = -\frac{1}{8Bc^2}\left(\frac{77}{80B^2c^4} + \frac{379}{120Bc^2} + 3\right) \tag{13b}$$

$$F_{12} = \frac{1}{80Bc^2}\left(\frac{77}{40B^2c^4} + \frac{329}{60Bc^2} + 3\right) \tag{13c}$$

$$F_{13} = -\frac{1}{120Bc^2}\left(\frac{21}{80B^2c^4} + \frac{67}{120Bc^2} + \frac{1}{3}\right) \tag{13d}$$

$$F_{22} = -\frac{1}{1280B^2c^4}\left(\frac{7}{2Bc^2}+3\right) \tag{13e}$$

$$F_{31} = \frac{1}{20B^2c^4}\left(\frac{7}{16Bc^2}+1\right) \tag{13f}$$

$$B = -\frac{1}{2e} \tag{13g}$$

By using the Chapman-Enscog procedure, the Navier-Stokes equations for compressible fluids can be derived. Expanding also the variables with respect to ε(<<1), corresponding the Knudsen number, as

$$f_a = f_a^{(0)} + f_a^{neq} = f_a^{(0)} + f_a^{(1)} + f_a^{(2)} + \cdots, \tag{14}$$

where non-equilibrium parts $f_a^{(l)} = O(\varepsilon^l)$ $(l = 1, 2, \cdots)$, and

$$\frac{\partial}{\partial t} \to \frac{\partial}{\partial t_1} + \frac{\partial}{\partial t_2}, \quad \frac{\partial}{\partial r_\alpha} \to \frac{\partial}{\partial r_{1\alpha}} \tag{15a,b}$$

where the partial differentiations $\partial/\partial t_l = O(\varepsilon^l)$ and $\partial/\partial r_l = O(\varepsilon^l)$ $(l = 1, 2, \cdots)$.

Substituting (14) and (15) into (2), we obtain up to $O(\varepsilon^2)$

$$\left(\frac{\partial}{\partial t_1}+\frac{\partial}{\partial t_2}\right)f_i^{(0)} + c_{i\alpha}\frac{\partial f_i^{(0)}}{\partial r_{1\alpha}} + \left(\frac{\partial f_i^{(1)}}{\partial t_1} + c_{i\alpha}\frac{\partial f_i^{(1)}}{\partial r_{1\alpha}}\right) = -\frac{1}{\phi}\left(f_i^{(1)} + f_i^{(2)}\right) \tag{16b}$$

We skip the detail, but we obtain the equation of continuity, the Navier-Stokes equation, and the energy equation for compressible fluids multiplying (2) by 1, $c_{i\alpha}$, and $c_{i\alpha}^2/2$, respectively

$$\frac{\partial \rho}{\partial t} + \frac{\partial}{\partial r_{1\alpha}}\left(\rho u_\alpha\right) = 0 \tag{17}$$

$$\frac{\partial}{\partial t}(\rho u_\alpha) + \frac{\partial}{\partial r_{1\beta}}\left(\rho u_\alpha u_\beta\right) = -\frac{\partial P}{\partial r_{1\alpha}} + \frac{\partial}{\partial r_{1\beta}}\mu\left(\frac{\partial u_\beta}{\partial r_{1\alpha}} + \frac{\partial u_\alpha}{\partial r_{1\beta}}\right) + \frac{\partial}{\partial r_{1\alpha}}\left(\lambda\frac{\partial u_\gamma}{\partial r_{1\gamma}}\right) \tag{18}$$

$$\begin{aligned}&\frac{\partial}{\partial t}\left(\rho e + \frac{1}{2}\rho u^2\right) + \frac{\partial}{\partial r_{1\alpha}}\left(\rho e + P + \frac{1}{2}\rho u^2\right)u_\alpha \\ &= \frac{\partial}{\partial r_{1\alpha}}\left(\kappa'\frac{\partial e}{\partial r_{1\alpha}}\right) + \frac{\partial}{\partial r_{1\alpha}}\left\{\mu u_\beta\left(\frac{\partial u_\beta}{\partial r_{1\alpha}} + \frac{\partial u_\alpha}{\partial r_{1\beta}}\right)\right\} + \frac{\partial}{\partial r_{1\alpha}}\left(\lambda\frac{\partial u_\beta}{\partial r_{1\beta}}u_\alpha\right)\end{aligned} \tag{19}$$

where the pressure P, the viscosity μ, the second viscosity λ, the thermal conductivity κ' are given as

$$P = \frac{2}{D}\rho e,\ \mu = \frac{2}{D}\rho e\phi,\ \lambda = -\frac{4}{D^2}\rho e\phi = -\frac{2}{D}\mu,\ \kappa' = \frac{2(D+2)}{D^2}\rho e\phi \tag{20a,b,c,d}$$

where $D = 2$ and 3 for two- and three-dimensional cases, respectively. In the above derivation of Navier-Stokes system, some deviation terms are omitted. See the Appendix for details.

3. New scheme for high Reynolds number flows

The relationship between the relaxation time ϕ and the kinetic viscosity μ is given in (20b), and the stability criterion of the collision term (RHS of (2)) demands that the time increment $\Delta t < \phi/2$, if we use the first order Euler scheme for the time integration: therefore the time increment must be very small for high Reynolds number flows and calculation efficiency will be poor.

A new term to change the relationship between ϕ and μ is added to (2) as

$$\frac{\partial f_i(t,\mathbf{r})}{\partial t} + c_{i\alpha}\frac{\partial f_i(t,\mathbf{r})}{\partial r_\alpha} - \frac{Ac_{i\alpha}}{\phi}\frac{\partial (f_i - f_i^{(0)})}{\partial r_\alpha} = -\frac{1}{\phi}\left[f_i(t,\mathbf{r}) - f_i^{(0)}(t,\mathbf{r}) \right] \tag{21}$$

where A is a positive constant, and other variables are the same as in (2). Equation (16) will be written as

$$\left(\frac{\partial}{\partial t_1} + \frac{\partial}{\partial t_2}\right) f_i^{(0)} + c_{i\alpha}\frac{\partial f_i^{(0)}}{\partial r_{1\alpha}} + \frac{\partial f_i^{(1)}}{\partial t_1} + (1 - \frac{A}{\phi})c_{i\alpha}\frac{\partial f_i^{(1)}}{\partial r_{1\alpha}} = -\frac{1}{\phi}\left(f_i^{(1)} + f_i^{(2)} \right) \tag{22}$$

In the same procedure as described above, the Navier-Stokes equations for a compressible fluid are obtained.

The viscosities and thermal conductivity are written as

$$\mu = \frac{2}{D}\rho e\tau(\phi - A),\ \lambda = -\frac{4}{D^2}\rho e\tau(\phi - A) = -\frac{2}{D}\mu,\ \kappa' = \frac{2(D+2)}{D^2}\tau\rho e(\phi - A) \tag{23a,b,c}$$

If a constant A is chosen an appropriate value, the time increment can be larger. The value of A can be chosen as large as 10^2 but we take 1/2 hereafter as the conventional LBM.

Here we consider equation (21) more in detail. The conventional lattice BGK model is written as

$$f_i\left(\mathbf{r} + \mathbf{c}\tau, t + \tau\right) = f_i\left(\mathbf{r}, \mathrm{t}\right) - \frac{1}{\phi}\left\{ f_i\left(\mathbf{r}, \mathrm{t}\right) - f_i^{(0)}\left(\mathbf{r}, \mathrm{t}\right) \right\} \tag{24}$$

This equation is discrete and in a finite difference form, and the continuous form obtained by the Taylor expansion to the second order of the time increment can be given as

$$\frac{\partial f_i}{\partial t} + c_{i\alpha}\frac{\partial f_i}{\partial r_\alpha} + \frac{1}{2}\tau c_{i\alpha}c_{i\beta}\frac{\partial^2 f_i}{\partial r_\alpha \partial r_\beta} + \tau c_{i\alpha}\frac{\partial^2 f_i}{\partial t \partial r_\alpha} + \frac{1}{2}\tau\frac{\partial^2 f_i}{\partial t^2} = -\frac{1}{\tau\phi}\left(f_i - f_i^{(0)} \right) \tag{25}$$

If we put the time increment $\tau = 1$ and employ the expansion (14) and (15), then we obtain for $O(\varepsilon)$

$$\frac{\partial f_i^{(0)}}{\partial t_1} + c_{i\alpha}\frac{\partial f_i^{(0)}}{\partial r_\alpha} = -\frac{1}{\phi} f_i^{(1)} \tag{26}$$

The additional term in (21) is expressed as

$$-Ac_\alpha \frac{\partial}{\partial r_\alpha}\frac{f_i^{(1)}}{\phi} = Ac_\alpha c_\beta \frac{\partial^2}{\partial r_\alpha \partial r_\beta} f_i^{(0)} + Ac_\alpha \frac{\partial^2}{\partial t_1 \partial r_\alpha} f_i^{(0)} \tag{27}$$

for $O(\varepsilon^2)$. If we take $A = 1/2$, (21) is identical with (25) except the terms

$$\frac{1}{2}\frac{\partial}{\partial t_1}\left(\frac{\partial f_i^{(0)}}{\partial t_1} + c_{i\alpha}\frac{\partial f_i^{(0)}}{\partial r_\alpha} \right) = \frac{1}{2}\frac{\partial}{\partial t_1}\left(-\frac{f_i^{(1)}}{\phi} \right) \tag{28}$$

These second-order terms have nothing to do with the derivation of the Navier-Stokes equations but they, especially the space derivative, change the

relationship between the viscosity and the relaxation parameter. Actually 1/2 appearing in, for example, the viscosity $\mu = \frac{2}{D}\rho e\tau(\phi - 1/2)$ in conventional LBM is due to discrete error, and just the factor of second term of Taylor expansion. This factor 1/2 corresponds with the inviscid limit of ϕ but this fact is only a coincidence. This error term also generates negative viscosity. The relaxation parameter ϕ should have been small to make the viscosity small, but owing to this negative viscosity ϕ can be a moderate value a little bit larger than 1/2 even for high Reynolds number flows. Introduction of the additional term in (21) means that this discrete error or negative viscosity is positively introduced into the model and this term reduces the viscosity for moderate value of ϕ.

4. Model having internal degrees of freedom

We propose a model having energy modes except the translation $G_a(t,\mathbf{r}) = f_a(t,\mathbf{r})E_a(t,\mathbf{r})$ to give the particle internal degree of freedom. The distribution function $G_a(t,\mathbf{r})$ is supposed to approach by collisions to its local equilibrium state $G_a^{(0)} = f_a^{(0)}E_a^{(0)}$ as the particle distribution functions do, and the evolution of G_a will be similar to (21) and expressed by

$$\frac{\partial G_a}{\partial t} + c_{a\alpha}\frac{\partial G_a}{\partial r_\alpha} - \frac{Ac_{i\alpha}}{\phi}\frac{\partial (G_a - G_a^{(0)})}{\partial r_\alpha} = -\frac{1}{\phi}\left(G_a - G_a^{(0)}\right) \tag{29}$$

In this model, the motion of the particles is calculated by (21) .

The local equilibrium distribution function is assumed to be given as the conventional form (11), and the unknown constants are determined as follows. The definitions of fluid density, momentum and momentum flux by $f_a^{(0)}$ are the same as (6), (7) and (9), respectively. The definition of the energy (8) will be replaced by

$$\frac{1}{2}\rho u^2 + \rho e = \sum_a \left(\frac{1}{2}f_a^{(0)}c_a^2 + G_a^{(0)}\right) = \sum_a \left(\frac{1}{2}c_a^2 + E_a^{(0)}\right)f_a^{(0)} \tag{30}$$

where kinetic energy except translation energy, that is, the rotation energy G_a is introduced. Similarly, (10) will be replaced by

$$\sum_a \left(\frac{1}{2}c_a^2 + E_a^{(0)}\right)f_a^{(0)}c_{a\alpha} = \left(\rho e + P + \frac{1}{2}\rho u^2\right)u_\alpha \tag{31}$$

At the local equilibrium stage all the particles have the same rotation energy as

$$E_a^{(0)} = E \qquad \text{for all } a \tag{32}$$

Then the constants F_a, B, and E are determined from (6), (7), (9), (30), (31) and (32).

The expression for the ratio of the specific heats γ in (1) will be written as

$$\gamma = \frac{D'+2}{D'} = \frac{D + D_E + 2}{D + D_E} \tag{33}$$

where D' is the total degree of freedom of the particle motion and D_E is the degree of freedom of the rotation. The energy at the equilibrium stage E is expressed as

$$E = \frac{D}{2}\left(\frac{D+2}{D} - \gamma\right)e \tag{34}$$

When the flow is two-dimensional $D = 2$ and the degree of freedom of the rotation D_E =1, for example, the energy E will be $E = e/3$ and other energy $2e/3$ will be distributed to the translation modes, and then each translation energy is $e/3$. Therefore the energy is equally distributed to each degree of freedom of motion. Of course, γ can be chosen any real value between 1 and 5/3 and D_E does not have to be integer. The constant B in (12g) and (13g) becomes

$$B = -\frac{1}{2(\gamma-1)e}\ , \tag{35}$$

but F_i are the same forms as in (12) and (13).

The macroscopic governing equations can be derived by a similar procedure stated above. The equations of continuity and motion are given in (17) and (18), respectively, and the pressure, the viscosity and the second viscosity are expressed using γ as

$$P = (\gamma-1)\rho e, \tag{36}$$

$$\mu = (\gamma-1)\rho e\tau(\phi - A), \tag{37}$$

$$\lambda = -(\gamma-1)^2\rho e\tau(\phi - A) = -(\gamma-1)\mu \tag{38}$$

Then the bulk viscosities $\chi = \lambda + \mu$ for two-dimensional flows and $\chi = \lambda + \frac{2}{3}\mu$ f or three-dimensional flows are not zero but are, respectively, $(2-\gamma)\mu$ and $\left(\frac{5}{3} - \gamma\right)\mu$.

The equation of energy, on the other hand, is derived by (21) and (29). The energy density G_a is also assumed to be expanded in powers of ε as

$$G_a = G_a^{(0)} + G_a^{neq} = f_a^{(0)}E_a^{(0)} + G_a^{(1)} + G_a^{(2)} + \cdots \tag{39}$$

where $G_a^{(l)} = O(\varepsilon^l)$ $(l = 1, 2, \cdots)$. Substituting (39) and multi-scale transformation (15a,b) into (21), we obtain

$$\left(\frac{\partial}{\partial t_1} + \frac{\partial}{\partial t_2}\right)f_a^{(0)}E_a^{(0)} + c_{a\alpha}\frac{\partial f_a^{(0)}E_a^{(0)}}{\partial r_{1\alpha}} + \frac{\partial G_a^{(1)}}{\partial t_1} + \left(1 - \frac{A}{\phi}\right)c_{a\alpha}\frac{\partial G_a^{(1)}}{\partial r_{1\alpha}} = -\frac{1}{\phi}\left(G_a^{(1)} + G_a^{(2)}\right) \tag{40}$$

The macroscopic equation of energy is obtained by multiplying (22) by the translation energy $c_a^2/2$ and adding (40), then summing up over all the particles. In this case non-equilibrium terms of energy are

$$\sum_a \frac{1}{2}f_a^{(l)}c_a^2 + \sum_a G_a^{(l)} = 0 \quad (l = 1, 2) \tag{41}$$

and we obtain

$$\frac{\partial}{\partial t}\sum_a\left(\frac{1}{2}c_a^2+E_a^{(0)}\right)f_a^{(0)}+\frac{\partial}{\partial r_{1\alpha}}\sum_a\left(\frac{1}{2}c_a^2+E_a^{(0)}\right)f_a^{(0)}c_{a\alpha}$$

$$-(\phi-A)\frac{\partial}{\partial r_{1\alpha}}\left(\frac{\partial}{\partial t_1}\sum_a\left(\frac{1}{2}c_a^2+E_a^{(0)}\right)f_a^{(0)}c_{a\alpha}+\frac{\partial}{\partial r_{1\beta}}\sum_a\left(\frac{1}{2}c_a^2+E_a^{(0)}\right)f_a^{(0)}c_{a\alpha}c_{a\beta}\right)=0 \tag{42}$$

Substitution of (11), (30) and (31) to the above equation leads the equation of energy presented in (19), in which, however, γ appears in the heat conductivity as

$$\kappa=\gamma\rho e\tau(\phi-A) \tag{43}$$

The sound speed c_s is given by

$$c_s=\sqrt{\gamma(\gamma-1)e} \tag{44}$$

The diffusive coefficients, the sound speed, and the equation of the equilibrium energy show that the model proposed above is consistent with the conventional model in which only the translation mode of the energy is considered. Moreover, this model considers the additional degrees of freedom of energy by (29) without changing the evolution equation of $f_a^{(0)}$; therefore it is very simple task to add the degree of freedom. The diffusion coefficient, the sound speed, and the equilibrium rotation energy are given by the same expressions in any models other than D2Q19 and D3Q39 models or models of other lattice shapes or those of other local equilibrium distribution functions $f_a^{(0)}$.

So far, $G_a=f_aE_a$ in (29) has been treated as a distribution function of the rotation energy, however it can be defined as a distribution function of any other kinetic energy. For instance, the degree of freedom is limited to the number of the dimension and it can be considered as the additional modes of translation energy for one- and two-dimensional space. In other words, it can be understood as distribution functions of any energy modes including translation that can not be expressed by the conventional models.

5. Calculation procedure

The time integration is performed by the second order Runge-Kutta method as

$$\left.\begin{aligned}f_i^{n+\frac{1}{2}}&=f_i^n+\frac{1}{2}\Delta t\left[-c_{i\alpha}\frac{\partial f_i^n}{\partial x_\alpha}+ac_{i\alpha}\frac{\partial}{\partial x_\alpha}\frac{f_i^n-f_i^{(0)n}}{\phi}-\frac{1}{\phi}\left(f_i^n-f_i^{(0)n}\right)\right]\\ f_i^{n+1}&=f_i^n+\Delta t\left[-c_{i\alpha}\frac{\partial f_i^{n+\frac{1}{2}}}{\partial x_\alpha}+ac_{i\alpha}\frac{\partial}{\partial x_\alpha}\frac{f_i^{n+\frac{1}{2}}-f_i^{(0)n+\frac{1}{2}}}{\phi}-\frac{1}{\phi}\left(f_i^{n+\frac{1}{2}}-f_i^{(0)n+\frac{1}{2}}\right)\right]\end{aligned}\right\} \tag{45}$$

and third-order upwind scheme is employed for space discretization as

$$c_x \frac{\partial f}{\partial x} = \begin{cases} c_x \dfrac{f(x-2\Delta x, y) - 6f(x-\Delta x, y) + 3f(x, y) + 2f(x+\Delta x, y)}{6\Delta x} & (c_x > 0) \\ c_x \dfrac{-f(x+2\Delta x, y) + 6f(x+\Delta x, y) - 3f(x, y) - 2f(x-\Delta x, y)}{6\Delta x} & (c_x < 0) \end{cases} \tag{46}$$

6. Some results

Some calculation results are presented using the proposed model having internal degrees of freedom for two- and three-dimensional flows and also conventional model for a monatomic gas.

6.1 Speed of sound

In order to check the validity of the proposed model, the sound speed is calculated for two-and three-dimensional models and compared to their theoretical value represented in (44). A one-dimensional tube is used, in which high pressure and low-pressure regions are separated at the initial stage as shown in Fig.1 and the separation is suddenly removed. The pressure ratio p_1 / p_2 is $1.0+10^{-10}$ and is so small that linear compression and expansion waves propagates at the sound speed instead shock or nonlinear expansion waves as shown in Figs. 2 a and 2b, where $\gamma = 1.4$ and $e = 1.0$, and

$$\Delta p = (p - p_2) / p_2 \tag{47}$$

The calculated and theoretical values of sound speed for variable γ are presented for D2Q21 and D3Q39 models in Figs 3 and 4, respectively, and the calculated values agree well to the theoretical ones.

6.2 Direct simulation of Aeolian tone

Direct simulation of acoustic waves emitted from a circular cylinder in a uniform flow has been calculated using a highly accurate finite difference method [17]. The same problem is performed using D3Q39 and D2Q21 models including the internal freedom of energy for $\gamma = 1.4$.

6.2.1 Aeolian tone by 3D39V model for Mach number 0.27

The cylindrical co-ordinate system is employed as shown in Fig.5 and the number of the grids is $201(r) \times 124(\theta) \times 5(z)$. The boundary condition is the uniform flow with velocity $u = 0.2$, internal energy $e_0 = 1.0$, therefore the Mach number is 0.27, and the density $\rho_0 = 1.0$ on the outer boundary whose radius is $r = 200d$ (d : the diameter of the cylinder). On the cylinder surface the velocity is zero and adiabatic. In the z-direction the periodic boundary condition is employed. The Reynolds number based on the cylinder diameter is 1000. The time increment $\Delta t = 0.01$.

The lift and the drag coefficients

$$C_D = \frac{D}{1/2\, \rho_0 U^2} \tag{48}$$

$$C_L = \frac{L}{1/2\,\rho_0 U^2} \tag{49}$$

are shown in Fig.6 and the Strouhal number determined from the variation of the lift is about 0.18.

A non-dimensional pressure fluctuation is defined by

$$\Delta p = (p - p_0)/p_0 \tag{50}$$

where p_0 is the initial pressure or the pressure on the outer boundary. The maximum and the minimum pressures are shown in Fig.7. The maximum pressure occurs near the stagnation point in the front of the cylinder and is almost constant. On the other hand, the minimum pressure occurs in the vortices of Karman Vortex Street and changes periodically. The difference between the maximum and the minimum pressures $\Delta p_{\max} - \Delta p_{\min}$ is of order of 10^{-1} and variation is of order of 10^{-2}. This variation of pressure occurs only vicinity of the circular cylinder, and the variation outside of the region is very small. Pressure variation due to the emission of the acoustic waves is also very small, but we can detect this periodic variation in the region far from the cylinder.

Pressure variation between $\Delta p = \pm 5\times 10^{-4}$ at non-dimensional time 158 is shown in Fig.8. In this figure red region is high-pressure region and blue region is of low pressure. Dipole-like emission of acoustic waves is seen and these waves travel with the sound speed and synchronized with the frequency of the lift on the cylinder due to the Karman vortex street. In the averaged value, the pressure on the upstream side is larger than that on the lee side of the cylinder, and the space of the neighboring rings is larger on the upstream side than that on the lee side due to the Doppler effect.

6.2.2 Aeolian tone by D2Q21 model for Mach number 0.027

It is very difficult to calculate low Mach number flows by the finite difference method based on the compressible Navie-Stokes equations. We present the results for very low Mach number flow in two-dimensional case because for low Mach number flows the flow velocity must small and it takes long time for three-dimensional calculation. The uniform velocity $u = 0.02$ and the internal energy $e_0 = 1.0$, then the Mach number of the flow is 0.027. The Reynolds number is 200. The outer boundary is set at $r = 2000d$, and the number of the grids is $601(r)\times 124(\theta)$, and the time increment is the same as that in Section 6.2.1.

The maximum and the minimum pressures are shown in Fig.9, and $\Delta p_{\max} - \Delta p_{\min}$ is smaller than those for $Ma = 0.27$ by two digits and 10^{-3}. The acoustic pressure field at non-dimensional time 183 is shown in Fig.10a between $\Delta p = \pm 3\times 10^{-7}$. The pattern is almost concentric circles and the Doppler effect is negligibly small. The pressure field subtracted by the averaged pressure is shown in Fig.10b and the dipole-like emission is more clearly seen.

If we take the diameter of the cylinder as 0.01m and the base pressure as 1.0×10^5 Pa and the temperature as 300K, then the flow velocity is about 9m/s, and the sound pressure at the point 1m distant from the cylinder in the direction perpendicular to the flow direction ($\theta=\pi/2$) is about 70dB. It is reasonable value.

6.2.3 Comparison with the results by Navier-Stokes based calculation

The acoustic pressures measured at the point $100\,d$ on the line perpendicular to the flow from the cylinder center are given in Fig.11. The left is the two-dimensional result of Navier-Stokes equations by Inoue [18] and the right is that by the present method. In the latter case, the number of the grids $401(r)\times124(\theta)$ the flow velocity $u=0.2$ and the internal energy is 50/63 and $\gamma=1.4$. The pressure becomes smaller if the number of the grids is too small in our simulation but 401 in r direction is enough. On the other hand the number of the grid in Inoue [18] is $871(r)\times503(\theta)$, and sixth–order -accurate compact Pade scheme and fourth-order Runge-Kutta method. The Reynolds number is 150 and the Mach number is 0.3 for both cases. These two results differ only by several percent.

This means that calculation load of our method is much lighter than that based on the Navier-Stokes equations.

6.3 Three-dimensional acoustic waves

In this paper, a uniform flow in x direction pasts a compact block as shown in Fig.12 is considered. The block is pentagon in the cross section because by breaking the symmetry of the flow at the early stage of calculation the flow oscillates much earlier and the sound will be more easily generated. The number of the grid is $129(x)\times131(y)\times140(z)$. Calculation region is $401d(x)\times401d(y)\times402d(z)$ where d is the length of the side of the block. The Mach number of the flow is 0.2 and the Reynolds number is 1000. The streamlines at a moment are shown in Fig. 13 , and the patterns of the acoustic pressure field are also shown in Fig.14.

The acoustic wave $\Delta p = O(10^{-7})$ is emitted in y direction as dipole like sound. Although the Mach number is moderate, the acoustic pressure is very small for full three-dimensional case.

7. Conclusion

Direct simulation of the aero acoustics is performed by the finite difference lattice Boltzmann method. A new scheme is proposed, and a model including the internal degree of freedom of the energy is also presented. The results for the Aeolian tone emitted from a circular cylinder agrees well with the Navier-Stokes equation based highly accurate result. It is shown that even very low Mach number flow at 0.027 reasonable result can be obtained. A full three-dimensional acoustic wave is also successfully calculated.

Appendix

In this appendix, we present the derivation of the Navier-Stokes system (17)-(19) emplying the Chapman-Enskog expansion.

From (3)-(5) and (6)-(8), it is clear that

$$\sum f_i^{(l)} = 0, \sum f_i^{(0)} c_{i\alpha} = 0, \sum \frac{1}{2} f_i^{(l)} c_{i\alpha}^2 = 0, \quad (l = 1, 2, 3\cdots) \tag{A1a,b,c}$$

Applying (14) and (15a,b) to (21), we obtain

$$\left(\frac{\partial}{\partial t_1} + \frac{\partial}{\partial t_2}\right) f_i^{(0)} + c_{i\alpha} \frac{\partial f_i^{(0)}}{\partial r_{i\alpha}} + \frac{\partial f_i^{(1)}}{\partial t_1} + \left(1 - \frac{A}{\phi}\right) c_{i\alpha} \frac{\partial f_i^{(1)}}{\partial r_{1\alpha}} = -\frac{1}{\phi}\left(f_i^{(1)} + f_i^{(2)}\right) \tag{A2}$$

A. Equation of continuity:

Multiplying unity to (22), and summing up all the particles in each lattice node we obtain

$$\frac{\partial \rho}{\partial t} + \frac{\partial}{\partial r_{1\alpha}}(\rho u_\alpha) = 0 \tag{A3}$$

Where (3),(4), (A1a) and (A1b) are used.

B. Equations of motion:

Multiplying $c_{i\alpha}$ to (22), and summing up all the particles in each lattice node we obtain

$$\frac{\partial}{\partial t}(\rho u_\alpha) + \frac{\partial}{\partial r_{1\beta}}\left(\rho u_\alpha u_\beta + p\delta_{\alpha\beta}\right) + \frac{\partial}{\partial t_1} \sum c_{i\alpha} f_i^{(1)} + \left(1 - \frac{A}{\phi}\right) \sum c_{i\alpha} c_{i\beta} \frac{\partial f_i^{(1)}}{\partial r_{1\beta}} = 0 \tag{A4}$$

where (9) is used. The third term on LHS is zero considering (A1b), but last term remains and this term represent the viscosity term.

From (26)

$$f_i^{(1)} = -\phi \left\{ \frac{\partial f^{(0)}}{\partial t_1} + c_{i\alpha} \frac{\partial f_i^{(0)}}{\partial r_{1\alpha}} \right\} \tag{A5}$$

Then this term can be written as

$$-(\phi - \mathrm{A}) \sum c_{i\alpha} c_{i\beta} \frac{\partial}{\partial r_{1\alpha}} \left\{ \frac{\partial f^{(0)}}{\partial t_1} + c_{i\gamma} \frac{\partial f_i^{(0)}}{\partial r_{1\gamma}} \right\} \tag{A6}$$

The first term, time derivative term, in curly bracket can be calculated by

$$\frac{\partial f^{(0)}}{\partial t_1} = \frac{\partial \rho}{\partial t_1} \frac{\partial f_i^{(0)}}{\partial \rho} + \frac{\partial u_\alpha}{\partial t_1} \frac{\partial f_i^{(0)}}{\partial u_\alpha} + \frac{\partial e}{\partial t_1} \frac{\partial f^{(0)}}{\partial e} \tag{A7}$$

and in this expression the time derivative terms $\frac{\partial\rho}{\partial t_1},\frac{\partial u_\alpha}{\partial t_1},\frac{\partial e}{\partial t_1}$ are transferred to space derivativess through the Euler equations because the first order continuous equation represents the Euler system. The terms $\frac{\partial f_i^{(0)}}{\partial\rho},\frac{\partial f_i^{(0)}}{\partial u_\alpha},\frac{\partial f_i^{(0)}}{\partial e}$ are obtained from (11) and (12) for two-dimensional model and (11) and (13) for three-dimensional model.

After a little manipulation, we obtain this viscosity term as

$$-(\phi-\mathrm{A})\sum c_{i\alpha}c_{i\beta}\frac{\partial}{\partial r_{i\alpha}}\left\{\frac{\partial f^{(0)}}{\partial t_1}+c_{ir}\frac{\partial f_i^{(0)}}{\partial r_{i\gamma}}\right\}=-\frac{\partial}{\partial r_{i\alpha}}\left[\frac{2}{3}\rho e(\phi-\mathrm{A})\left(\frac{\partial u_\alpha}{\partial u_\beta}+\frac{\partial u_\beta}{\partial u_\alpha}\right)\right]$$
$$-\frac{\partial}{\partial r_{i\alpha}}\left[\frac{4}{9}\rho e(\phi-\mathrm{A})\frac{\partial u_\gamma}{\partial r_{1\gamma}}\right]+E(\textit{deviation term}) \tag{A8}$$

Where the deviation term E is given

$$E=(\phi-\mathrm{A})\left[\frac{\partial^2}{\partial r_{1\beta}\partial r_{1\gamma}}\left(\rho u_\alpha u_\beta u_r\right)+\frac{\partial^2}{\partial r_{1\alpha}\partial r_{1\beta}}\left(\rho\frac{u^2}{2}u_\beta\right)+\frac{\partial^2}{\partial r_{1\beta}^2}\left(\rho\frac{u^2}{2}u\alpha\right)+\frac{\partial^2}{\partial r_{1\alpha}\partial r_{1\gamma}}\left(\rho\frac{u^2}{2}ur\right)\right] \tag{A9}$$

And the viscosity and the second viscosity are

$$\mu=\frac{2}{3}\rho e(\phi-A),\ \lambda=-\frac{4}{9}\rho e(\phi-A) \tag{A10a,b}$$

C. Energy equation:

Multiplying $\frac{c_{i\alpha}^2}{2}$ to (22), and summing up all the particles in each lattice node we obtain

$$\frac{\partial}{\partial t}\left(\rho\left(e+\frac{u^2}{2}\right)\right)+\frac{\partial}{\partial r_{1\alpha}}\left\{u_\alpha\left[\rho\left(e+\frac{u^2}{2}\right)+p\right]\right\}+\frac{\partial}{\partial t_1}\sum\frac{c_i^2}{2}f_i^{(1)}+\left(1-\frac{\mathrm{A}}{\phi}\right)\frac{\partial}{\partial r_{1\alpha}}c_{i\alpha}\frac{c_i^2}{2}f^{(1)}=0 \tag{A11}$$

The third term on LHS is zero considering (A1c) and the last tem represents the thermal diffusion, and, from the same procedure used in the equation of motions, this term is given as

$$-(\phi-\mathrm{A})\frac{\partial}{\partial r_{1\alpha}}c_{i\alpha}\frac{c_i^2}{2}\left[\frac{\partial f^{(0)}}{\partial t_1}+c_{i\alpha}\frac{\partial f_i^{(0)}}{\partial r_{1\alpha}}\right]$$
$$=-\frac{\partial}{\partial r_{1\alpha}}\left[\frac{10}{9}\rho e(\phi-A)\frac{\partial e}{\partial r_{1\alpha}}+\frac{2}{3}\rho e(\phi-A)u_\beta\left(\frac{\partial u_\alpha}{\partial r_\beta}+\frac{\partial u_\beta}{\partial r_{1\alpha}}\right)-\frac{4}{9}\rho e(\phi-A)u_\alpha\frac{\partial u_\beta}{\partial r_\beta}\right]-E' \tag{A12}$$

Where E' is the deviation term and

$$E'=-(\phi-\mathrm{A})\frac{\partial^2}{\partial r_{1\alpha}\partial r_{1\beta}}\rho u_\alpha u_\beta\frac{u^2}{2} \tag{A13}$$

And the heat conductiveity, the viscosity and the secondd viscosity are

$$\kappa'=\frac{10}{9}\rho e(\phi-A),\ \mu=\frac{2}{3}\rho e(\phi-A),\ \lambda=-\frac{4}{9}\rho e(\phi-A) \tag{A14a,b,c}$$

Our model has some deviation terms in equations of motion and energy, and these terms higher order of flow velocity or Mach number and second derivative terms, so that the error is small not only near the fixed body because the local Mach number is small but also in the regeon far from the body because the second derivative in flow velocity is generally small there. Therefore this model works well for whole flow field except the Mach number of the flow is so large.

The model proposed by Chen et.al. or Watari and Tsutahara [19] do not have such deviation terms. But the present model is very simple and tough in calculation and accurate enough, so we have used the present model for practical calculations.

References

[1] Frisch U, Hasslacher B, and Pomeau Y. Lattice gas automata for the Navier-Stokes equations, Complex Systems 1987; 1: 649-707.

[2] Wolfram S, Cellular automaton fluids 1; Basic Theory, J. Statistical Physics 1986; 45 :471-526.

[3] Rothman DH, Zalenski S, Lattice-gas cellular automata, Cambridge U.P. 1997.

[4] Chopard B, and Droz M, Cellular automata modeling of physical systems, Cambridge University Press 1998.

[5] McNamara G, Zanetti G, Use of the Boltzmann equation to simulate lattice-gas automata, Phys.Rev.Lett 1988; 61:2332-2335.

[6] Wolf-Gladrow DA, Lattice-gas cellular automata and lattice Boltzmann models, Lecture Notes in Mathematics, Springer 2000.

[7] Qian YH, Succi S, Orszag SA, Recent advances in lattice Boltzmann computing, Ann. Rev. of Comp. Phy. III, D. Stauffer ed. World Scientific, 19951;95-242.

[8] Chen S, Doolen GD, Lattice Boltzmann method for fluid flows, Ann. Rev. Fluid Mech., Ann. Rev. Inc. 1998.

[9] Succi S, The lattice Boltzmann equation for fluid dynamics and beyond, Oxford 2001.

[10]Abe T, Derivation of the lattice Boltzmann method by means of the discrete method for the Boltzmann equation, J. Comp. Phys 1997; 131: 241-246.

[11]He X, Luo L-S, A priori derivation of the lattice Boltzmann equation, Phys. Rev. E, 1997; 55 (6) :6333-6336.

[12]Alexander FJ., et al., Lattice Boltzmann thermohydro-dynamics, Phys. Rev. E 1993; 47:R2249- R2252,.

[13]Chen Y, et al., Thermal lattice Bhatnager Gross Krook model without nonlinear deviation in macrodynamic equations, Phys. Rev., E 1994; 50: 2776-2783.

[14]Tsutahara M, Takada N, Kataoka T, Lattice gas and lattice Boltzmann methods, Corona-sha 1999; in Japanese.

[15]Takada N, Tsutahara M, Proposal of Lattice BGK Model with Internal Degrees of Freedom in Lattice Boltzmann Method, Transactions of the Japan Society of Mechanical Engineers B, 1999; 65: 629: 92-99, in Japanese.

[16]Cao NS, Chen S, Jin S, Martinez D, Physical symmetry and lattice symmetry in the lattice Boltzmann method, Phys. Rev., E, 1997; 55: R21-R24.

[17]Lele SK, Computational aeroacoustics: A review, AIAA Paper 1997; 97-0018.

[18]Inoue O, Hatakeyama N, Sound generation by a two-dimensional circular cylinder in a uniform flow, J. Fluid Mech. 2002; 471:285-314.

[19]Watari M, Tsutahara M, Two-dimensional thermal model of the finite-difference lattice Boltzmann method with high spatial isotropy, Phys. Rev., E, 2003; 67: 036306-1-036306-7.

p	k	Velocity vector $\mathbf{c}_{pki} = \left(c_{pkix}, c_{pkiy}\right)$	$c_{pk} = \left\|\mathbf{c}_{pki}\right\|$
0	0	(0,0)	0
1	1	(1,0),(0,1),(-1,0),(0,-1)	1
1	2	(2,0),(0,2),(-2,0),(0,-2)	2
1	3	(3,0),(0,3),(-3,0),(0,-3)	3
2	1	(1,1),(-1,1),(-1,-1),(1,-1)	$\sqrt{2}$
2	2	(2,2),(-2,2),(-2,-2),(2,-2)	$2\sqrt{2}$

Table 1 Particles of D2Q21 model

p	k	Velocity vector $\mathbf{c}_{pki} = \left(c_{pkix}, c_{pkiy}, c_{pkiz}\right)$	$c_{pk} = \left\|\mathbf{c}_{pki}\right\|$
0	0	(0,0,0)	0
1	1	(1,0,0),(-1,0,0),(0,1,0),(0,-1,0),(0,0,1),(0,0,-1)	1
1	2	(2,0,0),(-2,0,0),(0,2,0),(0,-2,0),(0,0,2),(0,0,-2)	2
1	3	(3,0,0),(-3,0,0),(0,3,0),(0,-3,0),(0,0,3),(0,0,-3)	3
2	2	(2,2,0),(-2,2,0),(-2,-2,0),(2,-2,0),(0,2,2),(0,-2,2), (0,-2,-2),(0,2,-2),(2,0,2),(-2,0,2),(-2,0,-2),(2,0,-2)	$2\sqrt{2}$
3	1	(1,1,1),(-1,1,1),(-1,-1,1),(1,-1,1), (1,1,-1),(-1,1,-1),(-1,-1,-1),(1,-1,-1)	$\sqrt{3}$

Table 2 Particles of D3Q39 model

$\rho_1 = (1+1.0\times10^{-10})\rho_2$	ρ_2
$e_1 = e_2$	e_2
$P_1 = (1+1.0\times10^{-10})P_2$	$P_2 = (\gamma-1)\rho_2 e_2$

Fig.1 Initial stage in the duct for simulation of acoustic wave

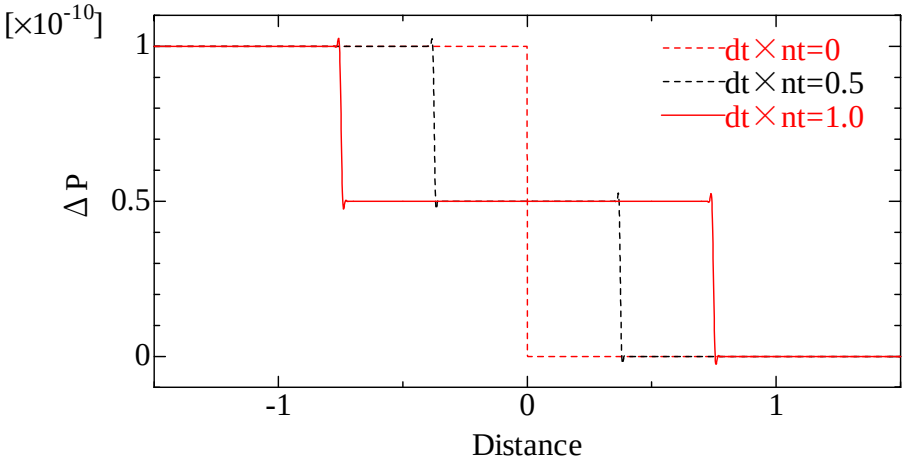

(a)

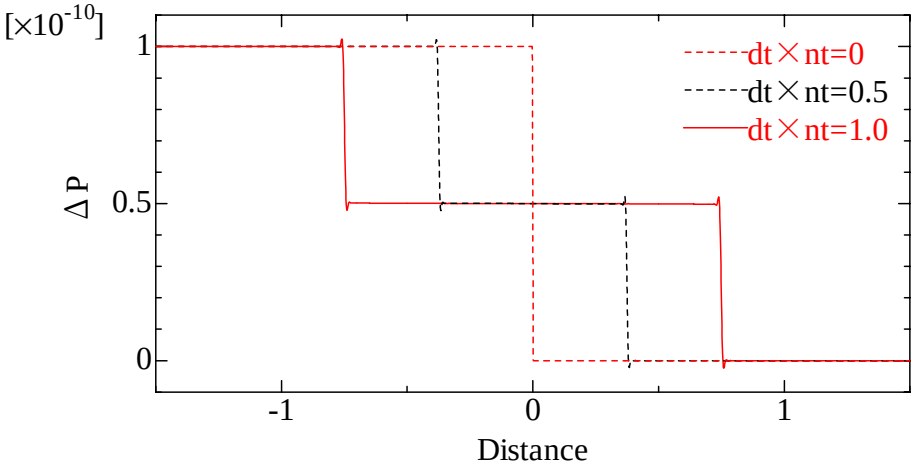

(b)

Fig.2 Propagation of expansion wave and compressive wave for (a) D2Q21 model and for (b) D3Q39 model with internal degree of freedom

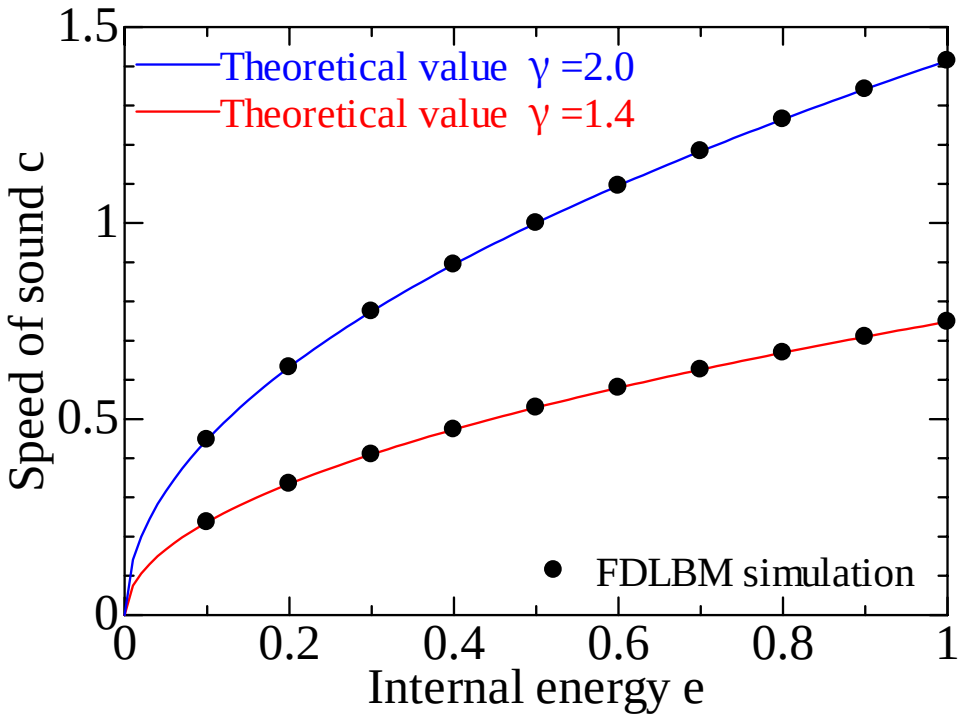

Fig.3 Calculation results of speed of sound by 2D21V model

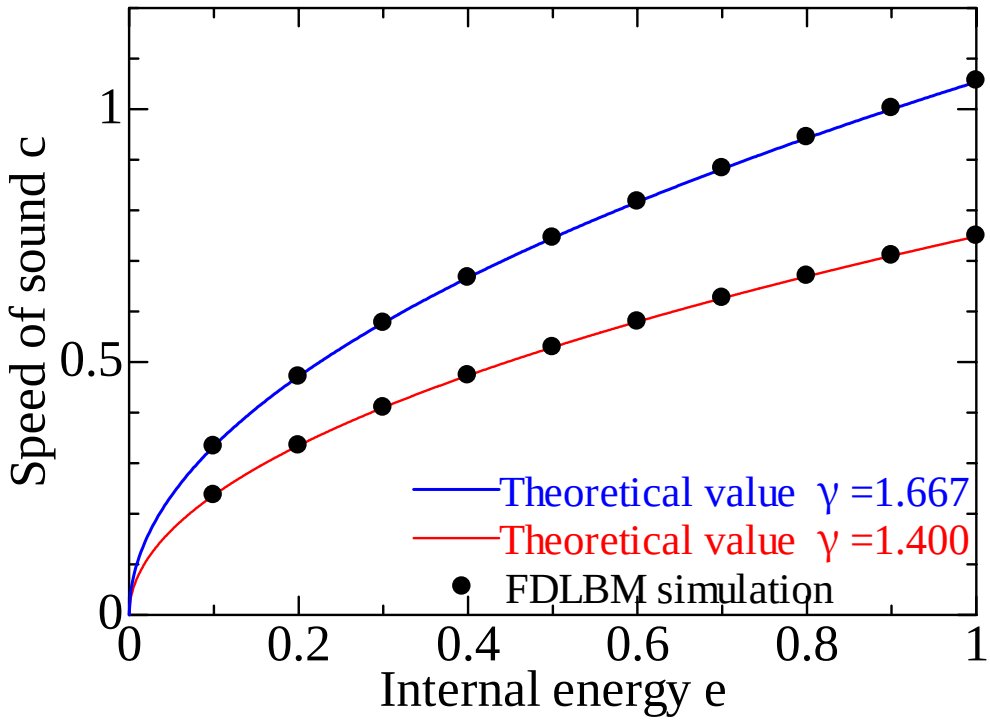

Fig. 4 Calculation results of sound speed for 3D39V model

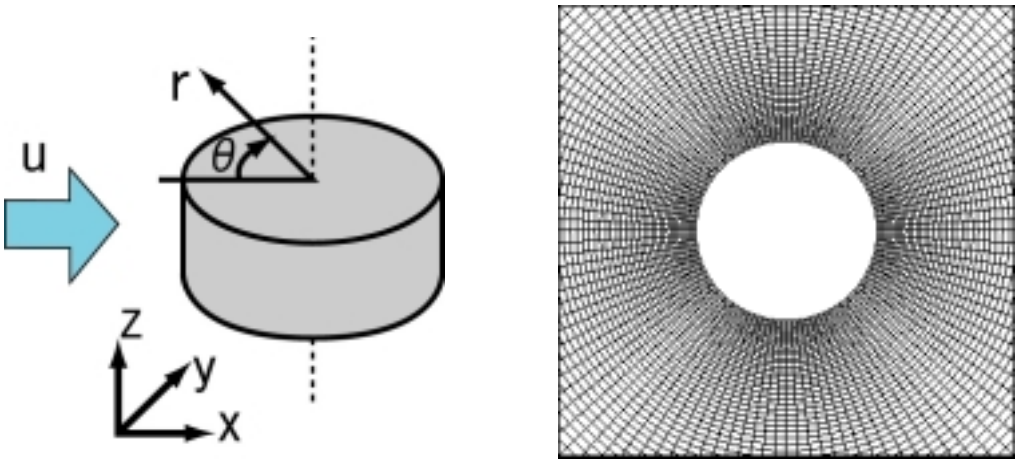

Fig.5 Flow past a circular cylinder and the cylindrical grid

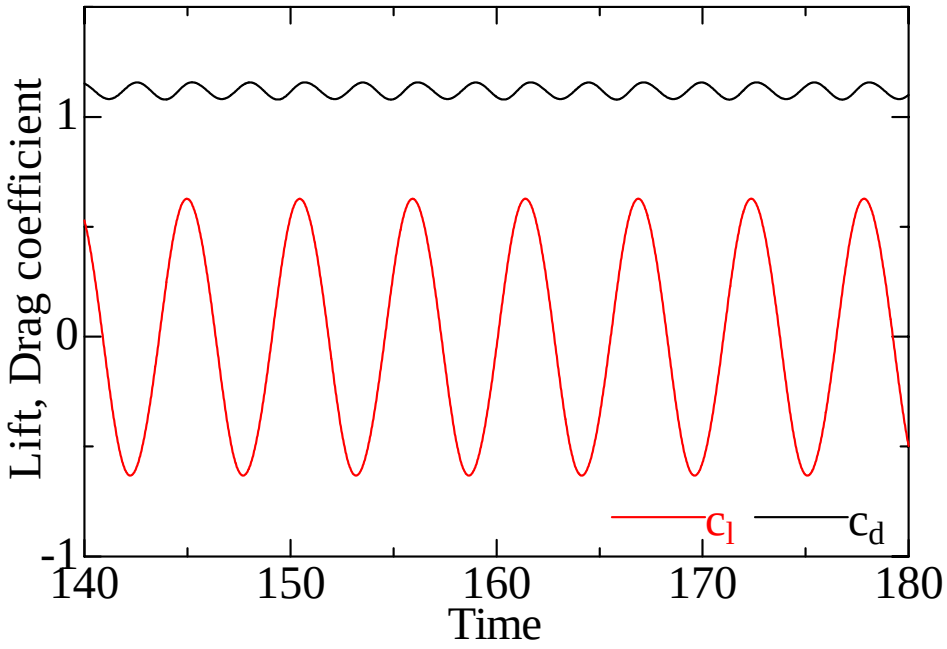

Fig.6 Time variation of Lift and Drag coefficients

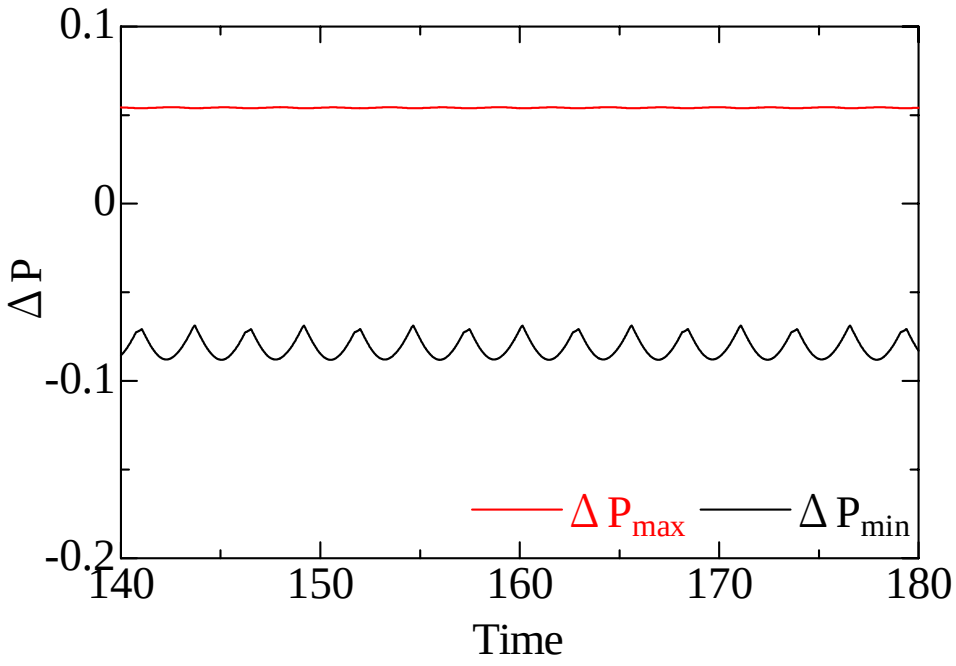

Fig.7 Time variation of maximum and minimum pressure for Ma=0.27

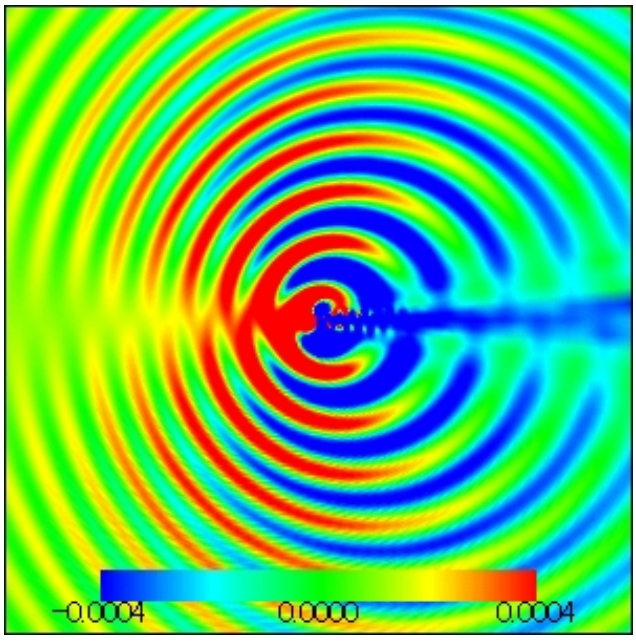

Fig.8 Acoustic pressure field of Aeolian tone (Re=1000, Ma=0.27, γ =1.4)

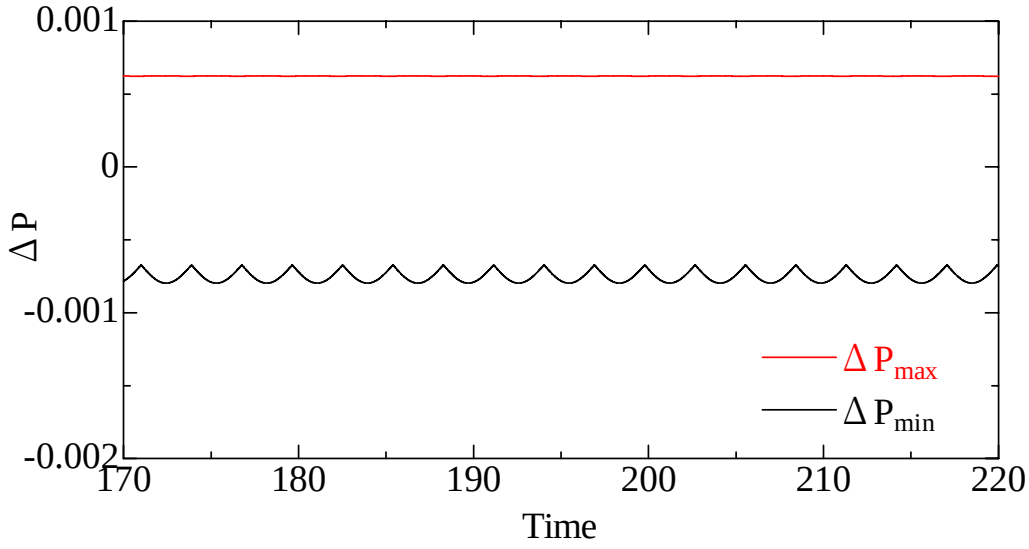

Fig.9 Time variation of maximum and minimum pressure for Ma=0.027

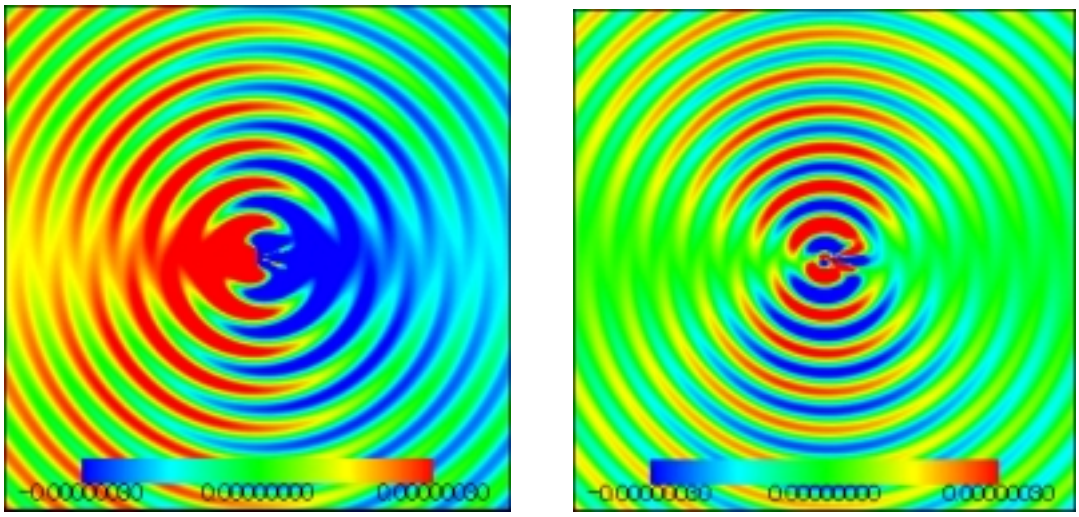

(a) (b)

Fig.10 Acoustic pressure field of Aeolian tone (Re=200, Ma=0.027, γ =1.4) in (a) and the pressure fluctuation subtracted by the averaged value in (b)

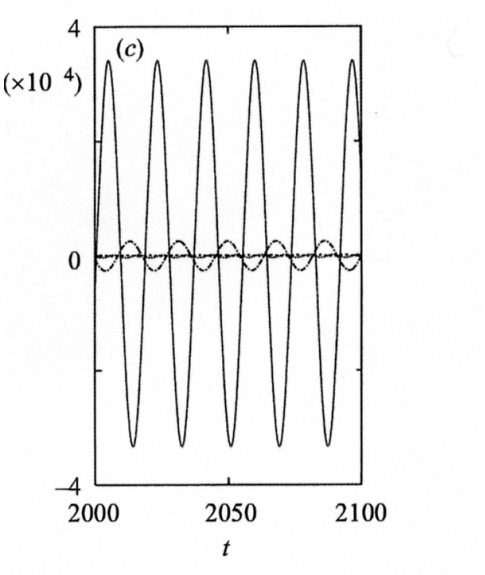

(a)

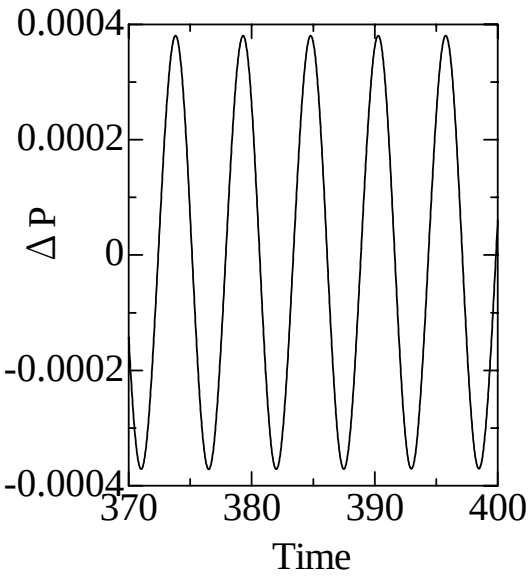

(b)

Fig.11 Comparison of pressure level (a) result by Navier-Stokes equation (b) result by present model

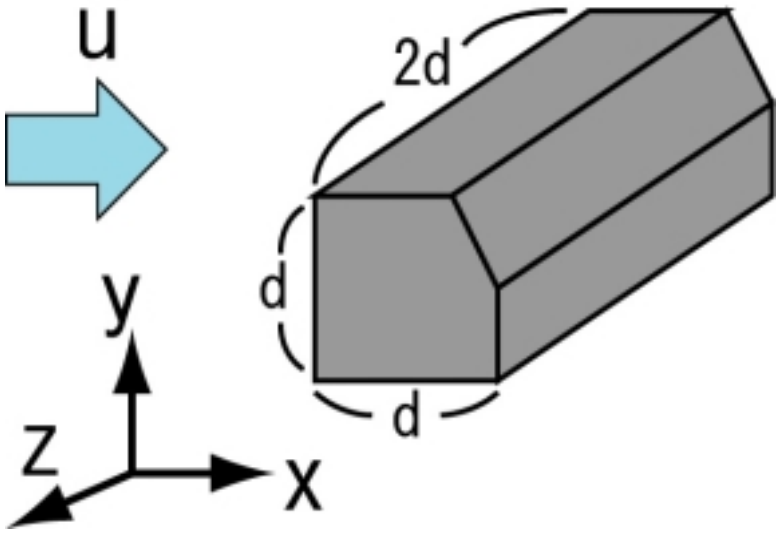

Fig.12 Flow past a block

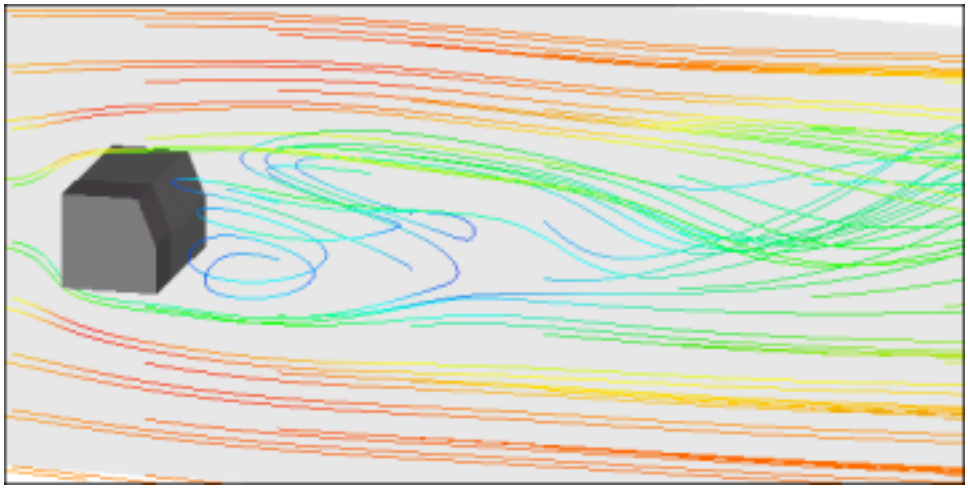

Fig.13 Streamlines past the block at non-dimensional time 150

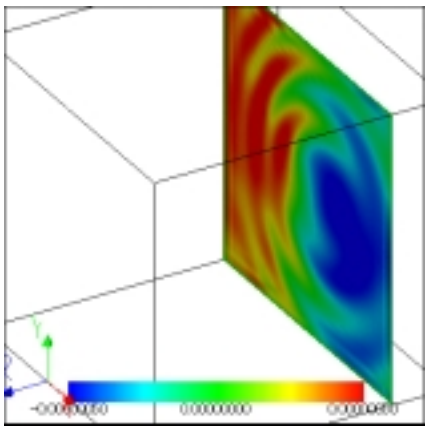

(a) x-y plane at t=180

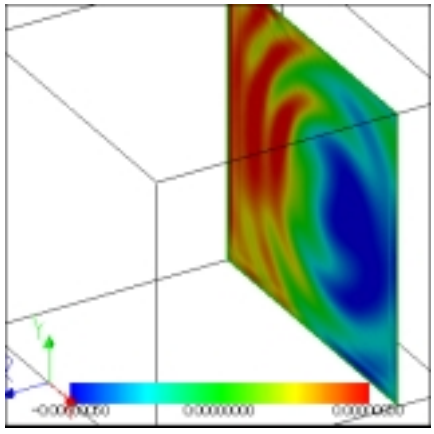

(b) x-y plane at t=184

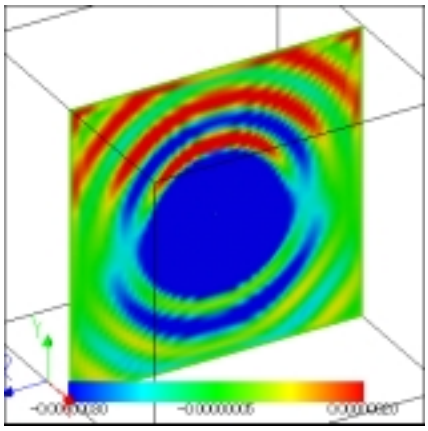

(c) y-z plane at t=180

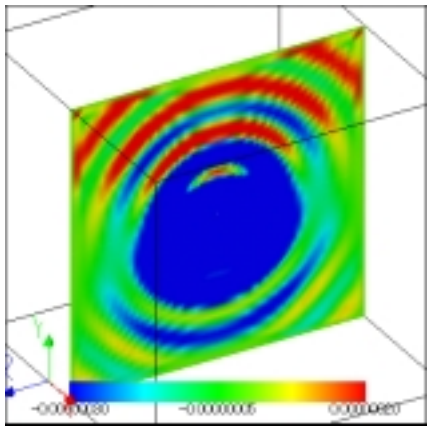

(d) y-z plane at t=184

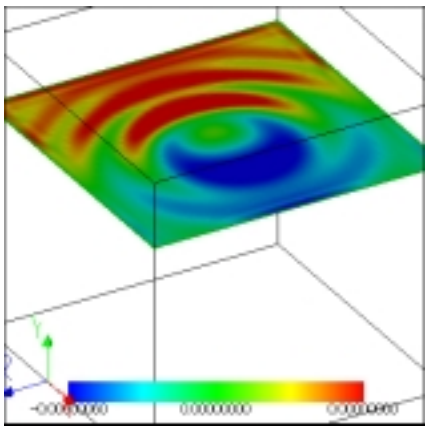

(e) z-x plane at t=180

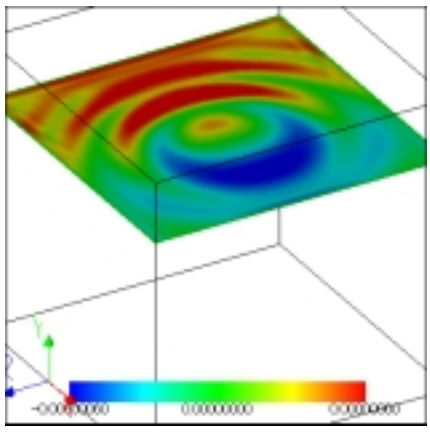

(f) z-x plane at t=184

Fig.14 Acoustic pressure distribution about the block, which is located at the center of the figures